Equation-Based Modelling: True Large Strain, Large Displacement And Anand's Plasticity Model with The ComSol Deformed Mesh Module

O. Toscanelli*,[1], V. Colla[1], M. Vannucci[1]
[1]Scuola Superiore S. Anna
*Viale Rinaldo Piaggio 34 - 56025 Pontedera (Pisa) Italy, tojfl@sssup.it

Abstract: In this work the solution of the structural problem obtained by mean of the velocity approach is presented. More in detail the balance and constitutive equations are expressed in Eulerian form, the mesh is not material. The approach is general, is suitable both for material boundary or no-material boundary and for a generic material model. The Hooke's elastic model and the Anand's plasticity model are considered. Some 2D and 3D cases are developed, with COMSOL, ANSYS and MSC-MARC, to study and verify this approach by respect to the structural problem.

Keywords: continuous, velocity, non-linear, plasticity, Anand

1 Introduction

The solution of the structural problem can be obtained using the velocity as dependent variable. So it is possible to model in a very general way the structural problem. Indeed, the velocity as dependent variable implies an incremental approach where the time variation of the various quantities must be defined. This is exactly the way in which the physical processes develop. Furthermore, the velocity approach allows:

1. no-material mesh (using FEM);
2. to model problems both with material boundary and/or no-material boundary;
3. to easily include generic and complex material model.

The velocity approach is especially suited to structural problems with large strain and displacement. In such problems, the possibility to use a no-material mesh can reduce powerfully the mesh-distortion. Across a material boundary there is not material flux, of this kind is the classical case of the structural study of a mechanic part. Across a no-material boundary there is material flux, this kind of boundary condition is used, for example, in continuous processes (like rolling).
The aim of this work is to study and verify the velocity approach. It is made with a Eulerian form of the equations, so the momentum balance is expressed by (1). The Hooke's elastic model (2) and the Anand's plasticity model (3) are considered. Both 2D and 3D cases are developed.

To handle and solve equations is used COMSOL with its Equation-Based Modelling and Deformed Mesh Module (to take the position and geometry variation). To verify the applied equations some simple cases are solved also with ANSYS and MSC-MARC. To study the velocity approach some cases are developed also to evaluate the model numerical behaviour.

2 Governing Equations

Only momentum balance and constitutive equations are considered. The temperature θ and the density ρ are constant and uniform. The momentum balance is expressed by

$$\rho\,\partial_t v_i + \rho\,\mathbf{v}\cdot\nabla v_i = \partial_j \sigma_{ij} + f_i \qquad (1)$$

The Hooke's elastic model is expressed by

$$\mathbf{T}^{\nabla} = \mathcal{L}\,\mathbf{D} \qquad (2)$$

The Anand's plasticity model [1] is expressed by

$$\mathbf{T}^{\nabla} = \mathcal{L}\,(\mathbf{D} - \mathbf{D}^{p}) \qquad (3)$$

Where
$\mathbf{v}$ is the velocity,
$\mathbf{f}$ is the body force,
$\mathbf{T}$ is the Cauchy stress tensor ($T_{ij} \equiv \sigma_{ij}$),
$T^{\nabla}_{ij} \equiv \partial_t \sigma_{ij} + v_l\,\partial_l \sigma_{ij} - W_{il}T_{lj} + T_{il}W_{lj}$,
$\mathcal{L} \equiv 2\mu I + [k - (2/3)\mu]\mathbf{1}\otimes\mathbf{1}$ is the fourth order isotropic elasticity tensor,

$\mathbf{D} \equiv \mathtt{sym}(\mathbf{L})$ is the stretching tensor ($L_{ij} \equiv \partial_j v_i$),
$\mathbf{W} \equiv \mathtt{skew}(\mathbf{L})$ is the spin tensor,
$\mathbf{D}^p \equiv \dot{\tilde{\epsilon}}^p (3/2)(\mathbf{T}'/\tilde{\sigma})$ is the flow rule,
$\mathbf{T}'$ is the deviator of the Cauchy stress tensor,
$\tilde{\sigma} = \sqrt{(3/2)\mathbf{T}' \cdot \mathbf{T}'}$ is the equivalent tensile stress,
$\dot{\tilde{\epsilon}}^p \equiv A \exp(-Q/(R\theta)) \left(\sinh(\xi\tilde{\sigma}/s)\right)^{1/m}$ is the flow equation,
$\dot{s} = h_0 \left|1 - s/s^*\right|^a \operatorname{sign}(1 - s/s^*)\, \dot{\tilde{\epsilon}}^p$ is the evolution equation with
$s^* = \tilde{s} \left[\dot{\tilde{\epsilon}}^p / A \exp(Q/(R\theta))\right]$
Where θ is the temperature in K.
The material parameters are: k, μ (Hooke and Anand), A, Q, m, ξ, h_0, a, $\tilde{s}$, s_0 (Anand).

3 Methods

To study and verify this velocity approach, simple 2D and 3D cases are simulated. In the present work, four kind of case are evaluated:

1. 2D axial-symmetric hollow sphere with internal hydrostatic pressure;
2. traction of a 3D beam;
3. bending of a 3D beam;
4. torsion of a 3D beam.

All cases are simulated with Hooke's material model, 1 and 4 also with Anand's material model. To study means to evaluate the numerical behaviour of the COMSOL models and their results. To verify means compare the results of the COMSOL models with those of the two commercial software ANSYS and MSC-MARC. To execute these tasks, deformed geometry and displacements, principal resultant, stresses and the balance between internal and external mechanical power are evaluated.

4 Numerical Model

The simulations are performed with the software:

1. COMSOL 3.5a;
2. ANSYS 11.0;
3. MSC-MARC 2005r3.

The simulations are performed on a 2 Quad-Core AMD Opteron(tm) Processor 2356 8GB RAM Linux WS. With the Hooke's material model the elements utilized in COMSOL are Lagrange-linear whereas in ANSYS and MSC-MARC are quadratic. With the Anand's material model MSC-MARC is not used and the elements utilized are linear both in COMSOL and in ANSYS. The elements are quadrilateral (2D) and hexahedron (3D) generated with a mapped mesh procedure. All the simulations are transient. With COMSOL, Equation-Based Modelling and Deformed Mesh Module are utilized.

For the coordinate system has been adopted the COMSOL nomenclature: $(x, y, z)_{\mathtt{ale}}$ is the spatial frame, $(X, Y, Z)_{\mathtt{ref}}$ is the reference frame.

`case 1`
The sphere has a concentric spherical hollow. The inner radius is 0.5, the outer one is 1.0 . The load is a pressure $p = 20\mathtt{MPa}\, t$ applied on the inner surface of the hollow. By symmetry, only a quarter of the diametrical section is modelled. The center is at $(0, 0, 0)_{\mathtt{ale}}$.

`cases 2-3-4`
The beam has a square section with a side of 0.05 and a length of 1.0. The x-axis is the beam axis. The beam ends are at $X = 0$ and $X = 1$. The loads are only on beam ends.

`case 3-4`
The beam ends are rigid surfaces.

`case 2`
The loads, for $t \in [0, 10]$, are:

$$\begin{aligned} v_x &= 0 \quad \text{at} \quad X = 0 \\ v_x &= 2t \quad \text{at} \quad X = 1 \end{aligned}$$

`case 3`
The loads, for $t \in [0, 1]$, are:

$$v_x = v_y = v_z = 0 \quad \text{at} \quad X = 0$$

$$\left.\begin{aligned} v_x &= v_{Px} - \dot{\alpha}\,(y - y_P) \\ v_y &= v_{Py} + \dot{\alpha}\,(x - x_P) \\ v_z &= 0 \end{aligned}\right\} \quad \text{at} \quad X = 1$$

Where $\mathbf{P}$ is the point of coordinates $(1, 0, 0)_{\mathtt{ref}} = (x_P, y_P, 0)_{\mathtt{ale}}$ and

$$\begin{aligned} x_P &= \sin(\alpha)/\alpha \\ y_P &= (1 - \cos(\alpha))/\alpha \\ v_{Px} &\equiv \dot{x}_P \\ v_{Py} &\equiv \dot{y}_P \\ \alpha &= \pi/6\, t^2 \end{aligned}$$

These loads at $X = 1$ are a rigid rotation-translation of the end beam around the point $\mathbf{P}$ with an angular velocity of $(0, 0, \dot{\alpha})$. The path of $\mathbf{P}$ is that it would have if the beam were bended in this way:

1. the length of the axis is constant;
2. the axis is an arc of circumference;
3. the sections that are orthogonal to the axis, at the initial time, remain orthogonal to it.

`case 4`
The loads, for $t \in [0, 1]$, are:

$$v_x = v_y = v_z = 0 \quad \text{at} \quad X = 0$$

$$\left.\begin{array}{rcl} v_x &=& 0 \\ v_y &=& -\dot{\alpha}\, z \\ v_z &=& +\dot{\alpha}\, y \end{array}\right\} \quad \text{at} \quad X = 1$$

$$\alpha = \pi\, t^2$$

These loads at $X = 1$ are a rigid rotation of the end beam around the point $(1, 0, 0)_{\texttt{ref}}$ with an angular velocity of $(\dot{\alpha}, 0, 0)$.

The material parameters are reported in the following tables.

Hooke	
E	70 MPa
ν	0.3

Anand	
E	105 GPa
ν	0.41
A	6.346 E+11 s^{-1}
Q	312.35 kJ/mol
m	0.1956
ξ	3.25
h_0	3093.1 MPa
a	1.5
$\tilde{s}$	121.1 MPa
R	8.314472 J/(mol K)
s_0	66.1 MPa

The Anand's parameters are pertinent to a BCC polycrystalline Fe-2% silicon alloy at a temperature $\theta = 1000\,\mathtt{C}$ [1].

5 Experimental Results

The results of the simulations have been analyzed and elaborated. They are reported in the next pictures and graphs.The resultant force $\mathbf{F}$, the resultant moment $\mathbf{M}$, the internal mechanical power $\mathcal{P}_{\texttt{int}}$ and the external mechanical power $\mathcal{P}_{\texttt{ext}}$ are calculated as:

$$\mathbf{F} = \int_{\mathcal{A}} \mathbf{t}\, d\mathcal{A}$$

$$\mathbf{M} = \int_{\mathcal{A}} \mathbf{OZ} \times \mathbf{t}\, d\mathcal{A}$$

$$\mathcal{P}_{\texttt{int}} = \int_{\Omega} \left[\sigma_{ij}\partial_i v_j - \rho\left(\partial_t v_i + v_j \partial_j v_i\right) v_i\right] d\Omega$$

$$\mathcal{P}_{\texttt{ext}} = \int_{\mathcal{A}} \mathbf{t} \cdot \mathbf{v}\, d\mathcal{A}$$

Where Ω is the mechanical part, $\mathcal{A}$ is the boundary on which loads are applied and $\mathbf{t} = \mathbf{t}(\mathbf{Z}, \mathbf{n})$ is the specific force applied on the surface $d\mathcal{A}$, that is centred on the point $\mathbf{Z}$ and that has the normal $\mathbf{n}$. The point $\mathbf{O} = (0, 0, 0)_{\texttt{ale}}$. The vector $\mathbf{u}$ is the displacement.

`case 1` Hooke
The displacements are reported on the point:

$$\mathbf{P}_1 = (0.5, 0)_{\texttt{ref}}$$

In fig.s 1, 2 is shown $\tilde{\sigma}$ respectively from COMSOL and ANSYS. In fig. 3 is shown $u_x(\mathbf{P}_1)$ from COMSOL and ANSYS.

`case 2-3-4`
The displacements are reported on the points:

$$\begin{aligned} \mathbf{P}_1 &= (1, 0, 0)_{\texttt{ref}} \\ \mathbf{P}_2 &= (1, 0.025, 0.025)_{\texttt{ref}} \\ \mathbf{P}_3 &= (0.5, 0.025, 0.025)_{\texttt{ref}} \end{aligned}$$

`case 2`
In this case, neglecting the inertial force, exists the analytical solution that is:

$$\begin{aligned} \varepsilon_{xx} &= \ln(1 + \partial_X u_x) \\ \sigma_{xx} &= E\varepsilon_{xx} \\ u_x(t, X, Y, Z) &= u_x(t, 1, 0, 0)\, X \end{aligned}$$

The displacement components u_x and u_y in the domain are shown in fig.s 4, 5. In fig. 6 are shown $u_x(\mathbf{P}_1)$ from COMSOL (`u1`) and from analytical solution (`u1_c`). In fig. 7 are shown $\sigma_{xx}(\mathbf{P}_1)$ from COMSOL (`s11`,`E1*e11`) and from analytical solution (`E*e11_c`). In fig. 8 are shown $u_y(\mathbf{P}_2)$ from COMSOl and MSC-MARC.

`case 3`
In fig.s 9, 10, 11 is shown $\tilde{\sigma}$ respectively from COMSOL, ANSYS and MSC-MARC. In fig. 12 is shown M_z from COMSOL, ANSYS and

MSC-MARC. In fig.s 13, 14 are shown respectively $u_x(\mathbf{P}_2)$ and $u_y(\mathbf{P}_2)$, from COMSOL, ANSYS and MSC-MARC. In fig. 15 are shown $\mathcal{P}_{\texttt{int}}$ and $\mathcal{P}_{\texttt{ext}}$ from COMSOL.

`case 4` Hooke
In fig.s 16, 17, 18 is shown $\tilde{\sigma}$ respectively from COMSOL, ANSYS and MSC-MARC. In fig. 19 is shown M_x from COMSOL, ANSYS and MSC-MARC. In fig.s 20, 21 are shown respectively $u_y(\mathbf{P}_2)$ and $u_z(\mathbf{P}_2)$, from COMSOL, ANSYS and MSC-MARC. In fig. 22 are shown $\mathcal{P}_{\texttt{int}}$ and $\mathcal{P}_{\texttt{ext}}$ from COMSOL.

`case 4` Anand
In fig.s 23, 25, is shown $\tilde{\sigma}$ respectively from COMSOL and ANSYS. In fig.s 24, 26, is shown s respectively from COMSOL and ANSYS. In fig. 27 is shown M_x from COMSOL and ANSYS. In fig.s 28, 29 are shown respectively $u_y(\mathbf{P}_3)$ and $u_z(\mathbf{P}_3)$, from COMSOL and ANSYS. In fig. 30 are shown $\mathcal{P}_{\texttt{int}}$ and $\mathcal{P}_{\texttt{ext}}$ from COMSOL.

6 Discussion

The deformed geometry obtained from COMSOL is that foreseen. The displacements $\mathbf{u}$ from COMSOL, ANSYS and MSC-MARC, are in very good agreement. The stresses and the principal resultant M_z, M_x from COMSOL. ANSYS and MSC-MARC, are in good agreement. The state variables s from COMSOL and ANSYS are in good agreement. In the case 2 there is a very good agreement between COMSOL and analytical solution. The very good agreement between $\mathcal{P}_{\texttt{int}}$ and $\mathcal{P}_{\texttt{ext}}$, demonstrate the goodness of the COMSOL simulations.

7 Conclusions

The solution (COMSOL) of the velocity approach equations is not problematic (i.e. are not necessary special numerical treatment). The agreement of the COMSOL results with those of ANSYS,MSC-MARC and analytical solution, demonstrate, within the limits of this preliminar work, the suitability of the velocity approach equations to solve the structural problem.

8 Use of COMSOL Multiphysics

COMSOL Equation-Based Modelling and Deformed Mesh Module are tools very suitable to solve this type of problem, not only for writing the necessary, and not standard, equations, but also for adding special terms to correct eventual numerical problems.

9 Figures

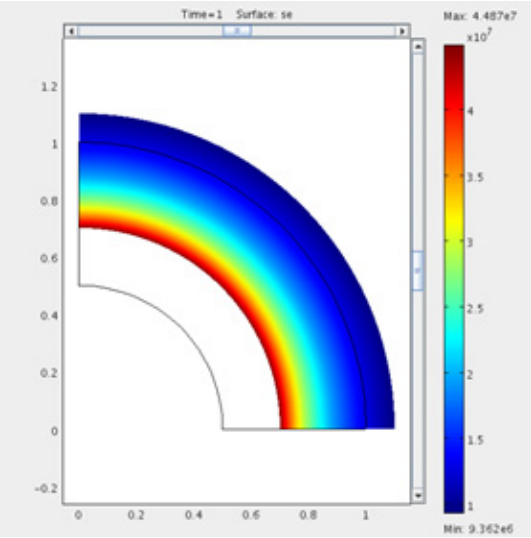

Figure 1: COMSOL 2D Hooke $\tilde{\sigma}$

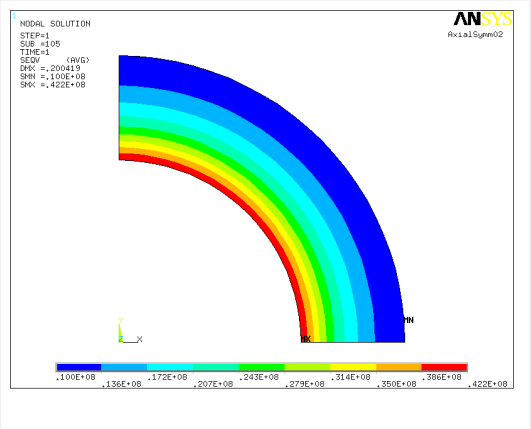

Figure 2: ANSYS 2D Hooke $\tilde{\sigma}$

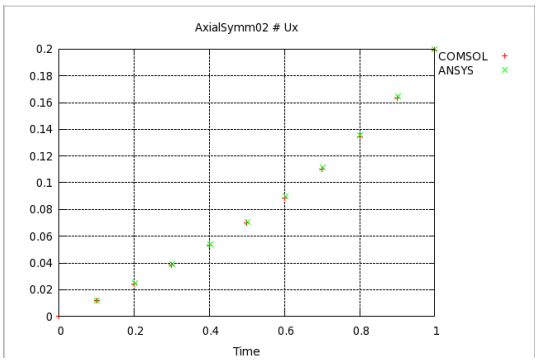

Figure 3: 2D Hooke $u_x(\mathbf{P}_1)$

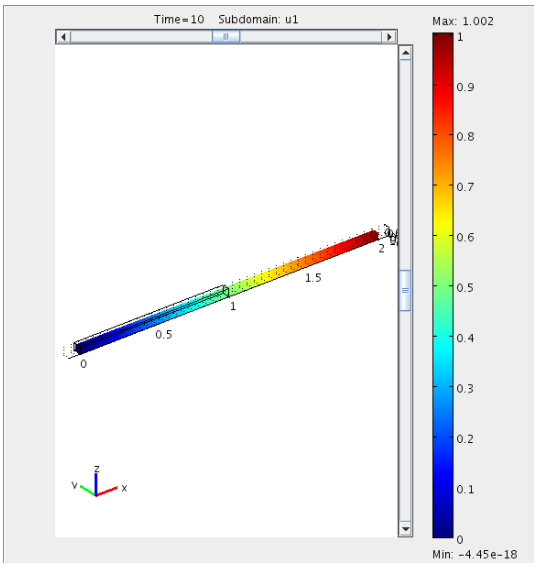

Figure 4: COMSOL traction Hooke u_x

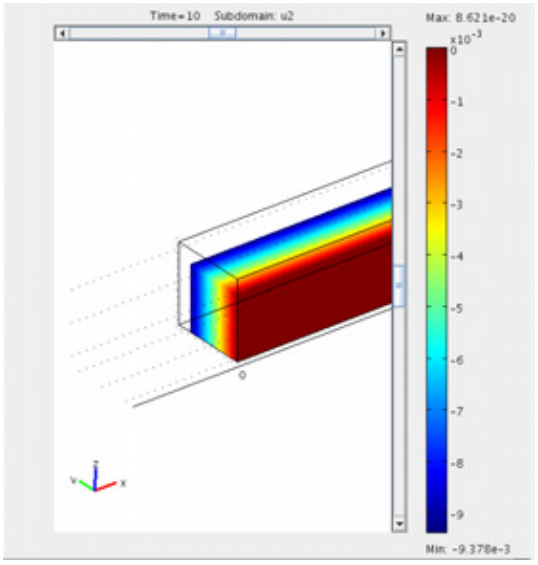

Figure 5: COMSOL traction Hooke u_y

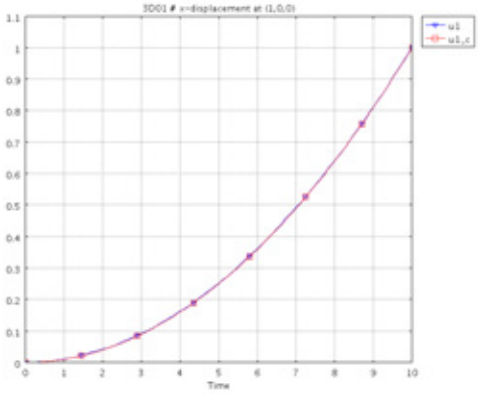

Figure 6: traction Hooke $u_x(\mathbf{P}_1)$

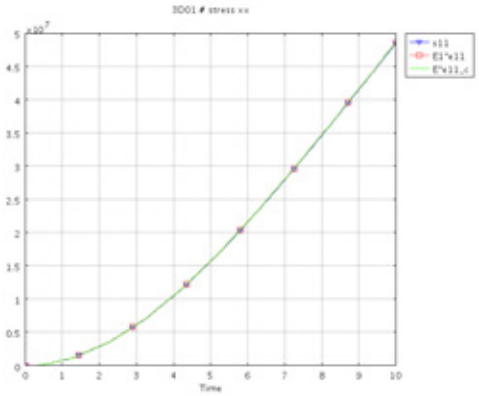

Figure 7: traction Hooke $\sigma_{xx}(\mathbf{P}_1)$

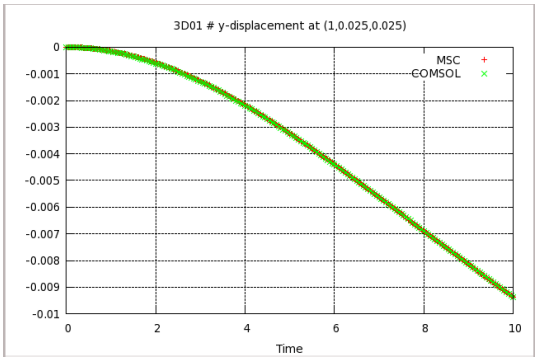

Figure 8: traction Hooke $u_y(\mathbf{P}_2)$

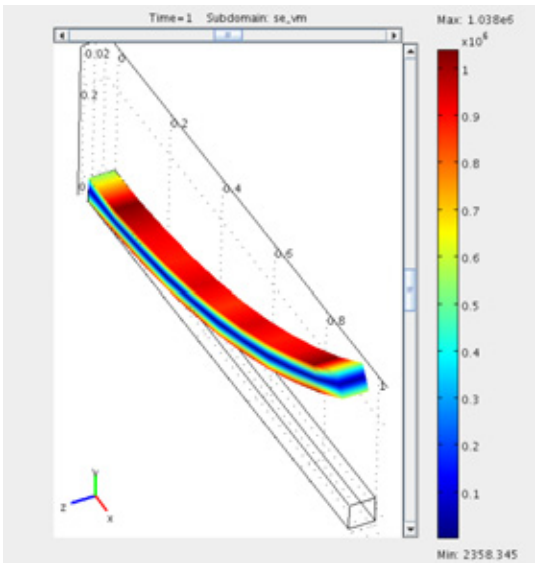

Figure 9: COMSOL bending Hooke $\tilde{\sigma}$

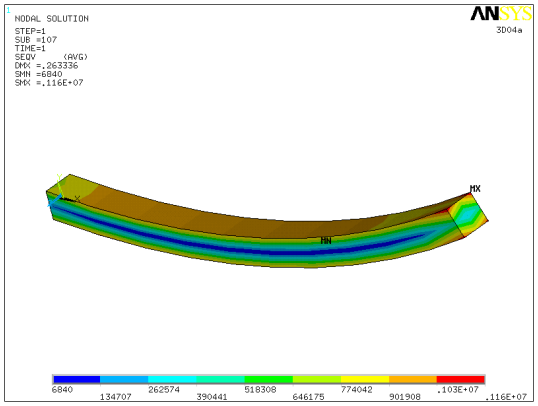

Figure 10: ANSYS bending Hooke $\tilde{\sigma}$

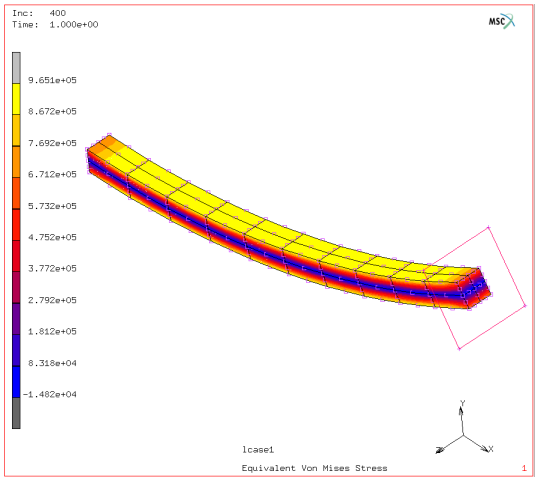

Figure 11: MSC-MARC bending Hooke $\tilde{\sigma}$

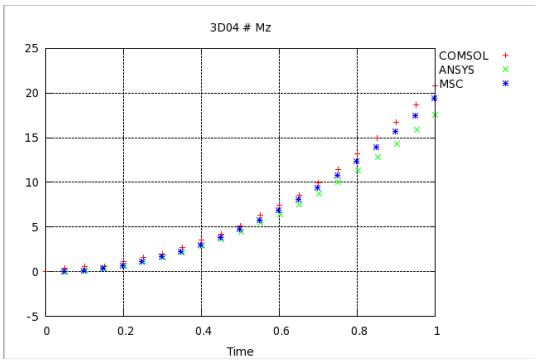

Figure 12: bending Hooke M_z

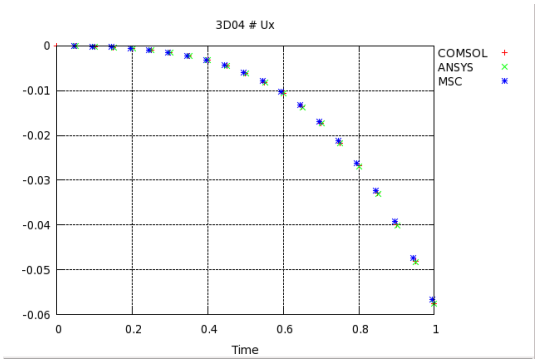

Figure 13: bending Hooke $u_x(\mathbf{P}_2)$

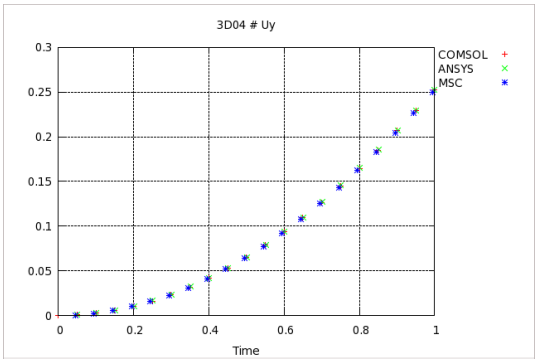

Figure 14: bending Hooke $u_y(\mathbf{P}_2)$

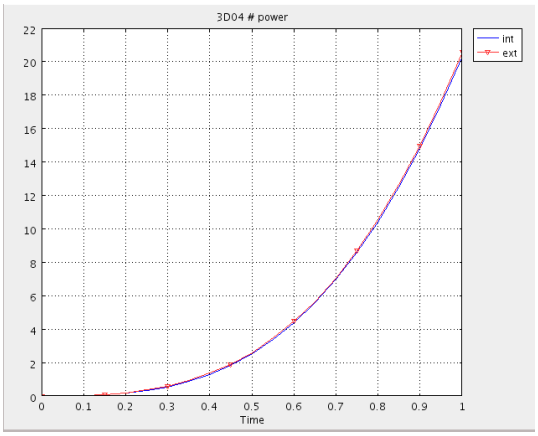

Figure 15: COMSOL bending Hooke $\mathcal{P}_{\text{int}}$ $\mathcal{P}_{\text{ext}}$

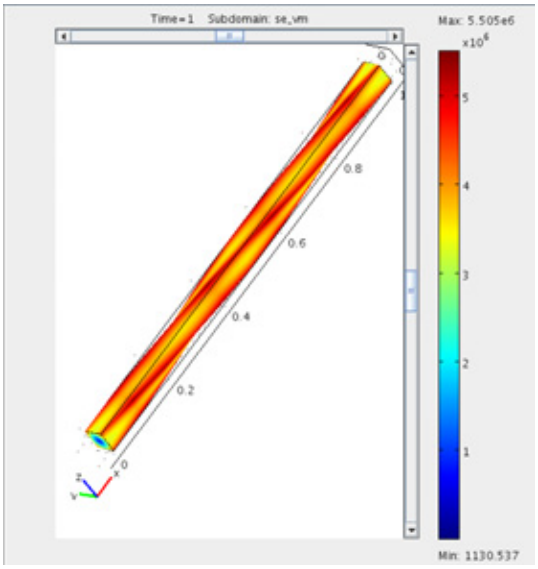

Figure 16: COMSOL torsion Hooke $\tilde{\sigma}$

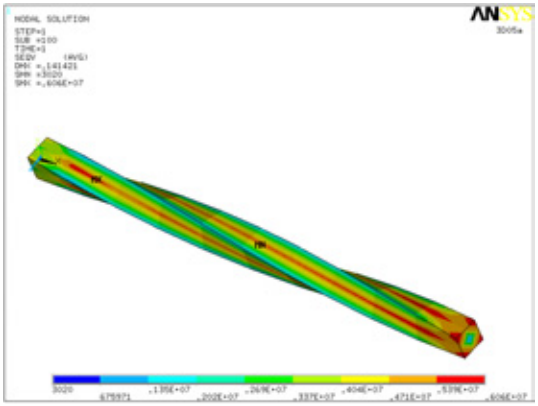

Figure 17: ANSYS torsion Hooke $\tilde{\sigma}$

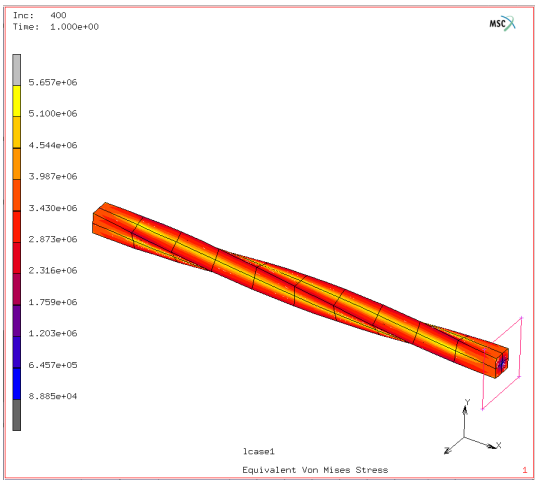

Figure 18: MSC-MARC torsion Hooke $\tilde{\sigma}$

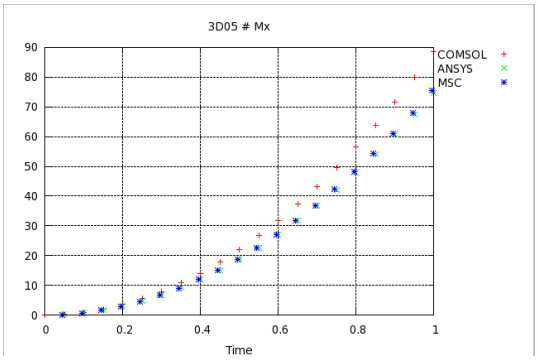

Figure 19: torsion Hooke M_x

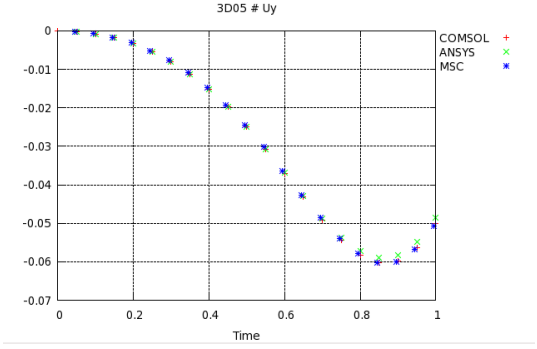

Figure 20: torsion Hooke $u_y(\mathbf{P}_2)$

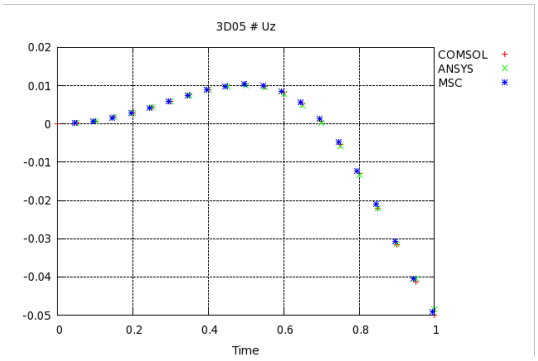

Figure 21: torsion Hooke $u_z(\mathbf{P}_2)$

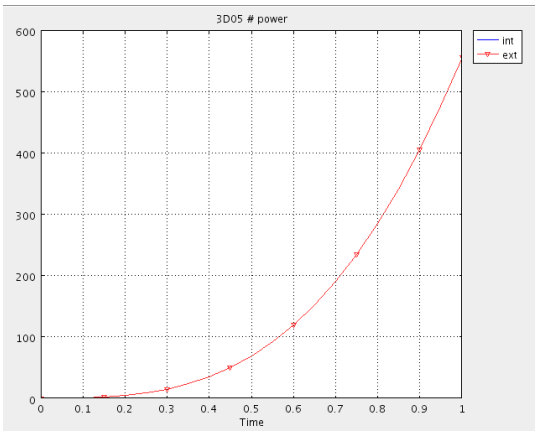

Figure 22: COMSOL torsion Hooke $\mathcal{P}_{\text{int}}$ $\mathcal{P}_{\text{ext}}$

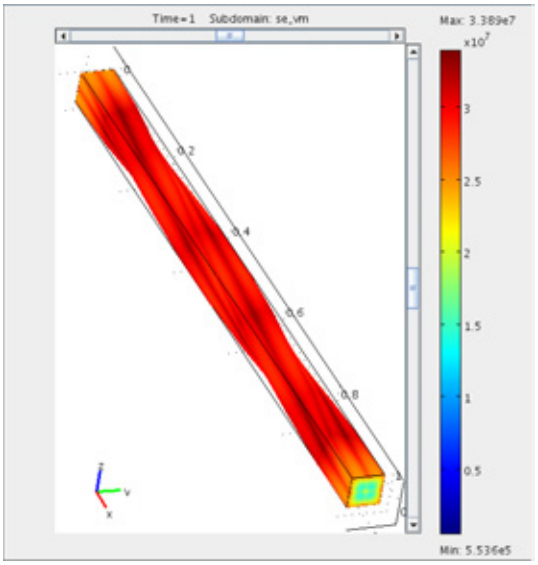

Figure 23: COMSOL torsion Anand $\tilde{\sigma}$

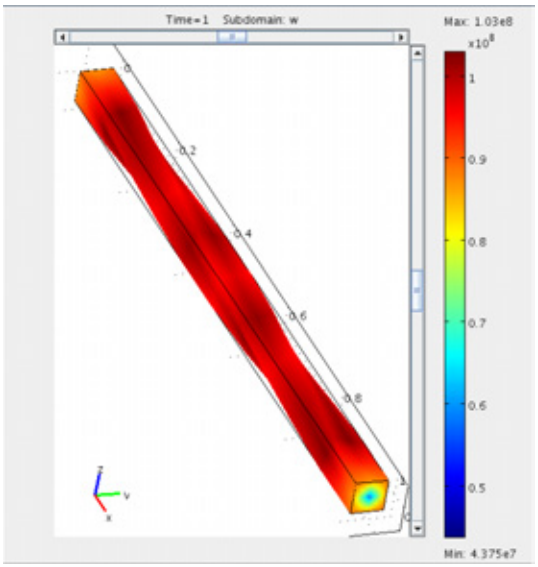

Figure 24: COMSOL torsion Anand s

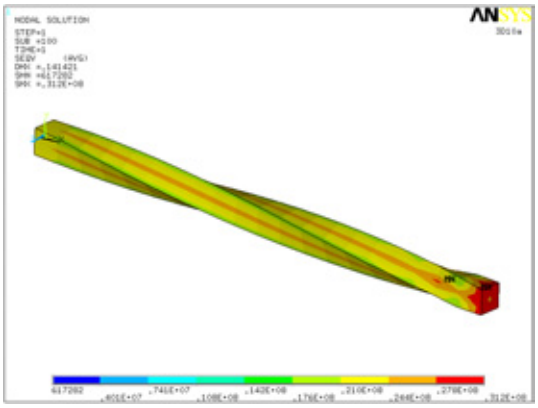

Figure 25: ANSYS torsion Anand $\tilde{\sigma}$

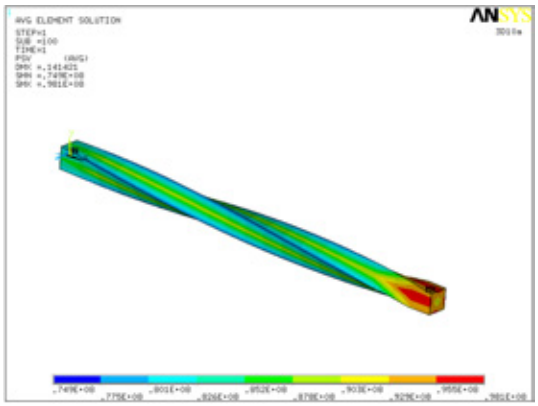

Figure 26: ANSYS torsion Anand s

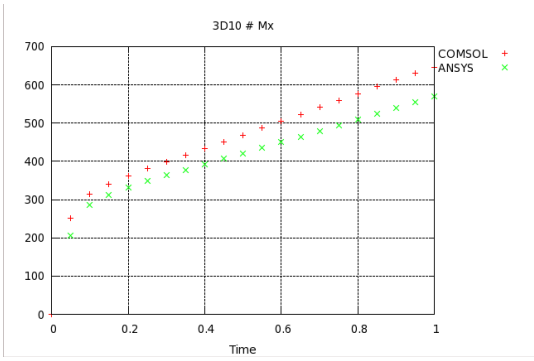

Figure 27: torsion Anand M_x

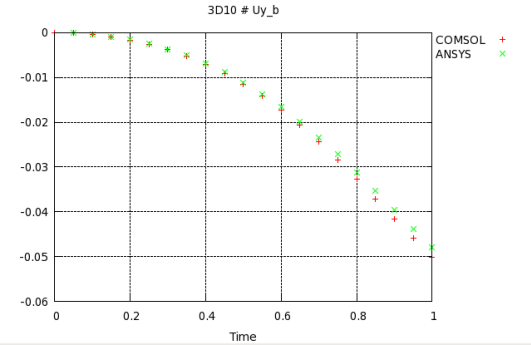

Figure 28: torsion Anand $u_y(\mathbf{P}_3)$

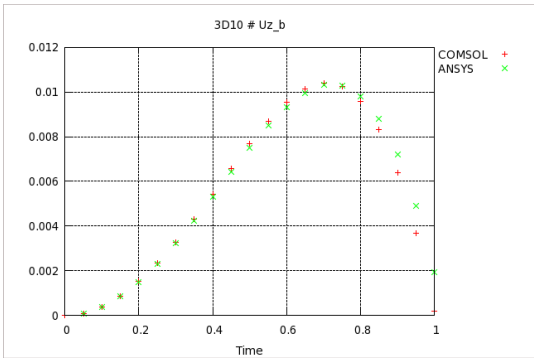

Figure 29: torsion Anand $u_z(\mathbf{P}_3)$

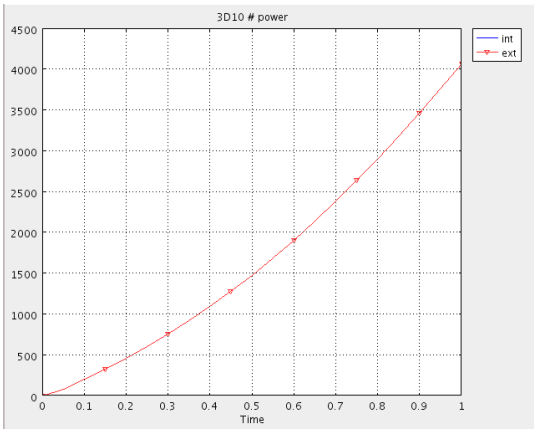

Figure 30: COMSOL torsion Anand $\mathcal{P}_{\mathtt{int}}$ $\mathcal{P}_{\mathtt{ext}}$

References

[1] Kwon H. Kim Stuart B. Brown and Lallit Anand, *An internal variable constitutive model for hot working of metals*, International Journal of Plasticity **5** (1989), 95–130.